THEORETICAL AND APPLIED MECHANICS
Volume 44 (2017) Issue 2, 237–254 DOI: https://doi.org/10.2298/TAM171002015O

THE BRACHISTOCHRONIC MOTION OF A VERTICAL DISK ROLLING ON A HORIZONTAL PLANE WITHOUT SLIP

Aleksandar Obradović, Slaviša Šalinić, and Radoslav Radulović

This work is dedicated to the memory of the late Professor Aleksandar Bakša

ABSTRACT. This paper deals with the brachistochronic motion of a thin uniform disk rolling on a horizontal plane without slip. The problem is formulated and solved within the frame of the optimal control theory. The brachistochronic motion of the disk is controlled by three torques. The possibility of the realization of the brachistochronic motion found in presence of Coulomb dry friction forces is inspected. Also, the influence of values of the coefficient of dry friction on the structure of the extremal trajectory is analyzed. Two illustrative numerical examples are provided.

1. Introduction

In Fig. 1, a thin uniform circular disk (also called coin) rolling without slip on a fixed horizontal plane coinciding with the coordinate plane Oxy of the inertial Cartesian reference frame $Oxyz$ is shown. The disk is of mass m and radius r, where G represents the mass center of the disk and C is the contact point of the disk with the plane. The curve L shown in Fig. 1 represents the contact-trajectory curve (also called the contact loci) on the plane Oxy.

A moving Cartesian frame $G\xi\eta\zeta$ is chosen in such way that during the motion of the disk the η-axis lying in the plane of the disk is parallel to the plane Oxy, the ζ-axis coincides with the direction CG, and the ξ-axis is perpendicular to the plane of the disk. The position of the mass center G relative to the frame $Oxyz$ is determined by the Cartesian coordinates x_G, y_G, and z_G, whereas the angular orientation ot the disk with respect to $Oxyz$ is described by the three angles ϕ, θ, and ψ . In many text books [1–8] the disk considered is often taken as an illustrative example in solving various problems of kinematics and dynamics of constrained mechanical systems

2010 *Mathematics Subject Classification:* 70E18, 70Q05.
Key words and phrases: brachistochronic motion, nonholonomic constraints, Coulomb dry friction, optimal control, rolling without slip.

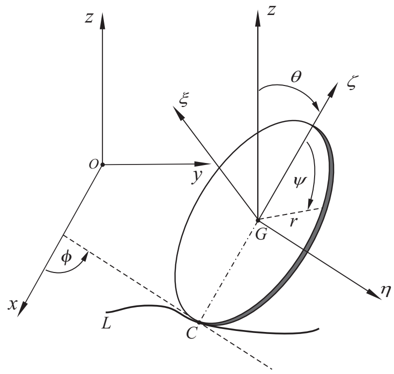

FIGURE 1. Rolling of a thin uniform circular disk over a horizontal plane.

with non-holonomic constraints. Also, a large number of works deal exclusively with solving kinematics and dynamics problems related to a thin disk rolling on a horizontal plane without slip (see e.g., [9–15]). Paper [16] considers the motion of a thin disk rolling without slip on an arbitrary rigid surface. On the other hand, in the literature available, the papers discussing the problem of brachistochronic motion of the disk consider the problem of seeking the curve lying in the vertical plane along which the disk, rolling without slip, is descending from a specified initial position to a specified terminal position for a minimum time (see [17–19]). Identical problem but for a circular cylinder is studied [20, 21]. Also, in these papers conditions of realizability of rolling without slip and separations in presence of the Coulomb dry-friction forces are considered. Note that in the paper [22], the brachistochronic motion of a conservative dynamical system as well as the geometrical characteristics of the regions of the possible brachistochronic motion of the systems are considered.

This paper considers the brachistochronic motion of a thin uniform disk rolling without slip on a horizontal plane. Such case has not been considered in the literature available to date. Like in [17–21], the analysis was performed of the realizability condition of the brachistochronic motion of the disk in the presence of the Coulomb dry-friction forces. Numerical examples are provided.

2. Differential equations of motion of the rolling disk

Let us consider the case of the disk shown in Fig. 1 for which one has $\theta(t) \equiv 0$. This means that the disk rolls without slip while remaining vertical on the plane Oxy, as it is shown in Fig. 2. Note that in this section, for the completeness of the exposition and for the need of adapting notation for the exposition in the following sections, a lot of well-known material related to the kinematics and dynamics of the considered disc, which can be found in the literature cited in this paper, is presented. Let us denote by $\mathbf{i}$, $\mathbf{j}$, and $\mathbf{k}$ the unit vectors of the axes x, y, and z, respectively. Also, $\boldsymbol{\lambda}$, $\boldsymbol{\mu}$, and $\boldsymbol{\nu}$ represent the unit vectors of the axes ξ, η, and ζ, respectively.

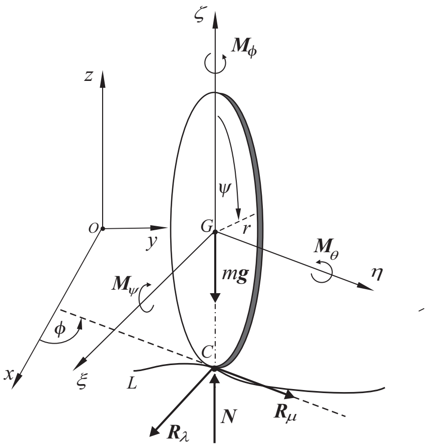

FIGURE 2. A vertical thin rolling disk whose motion is controlled by three torques.

The disk is acted on by the weight $m\mathbf{g}$ and the couples of forces of the torques $\mathbf{M}_\phi = M_\phi \mathbf{k}$, $\mathbf{M}_\psi = -M_\psi \boldsymbol{\lambda}$, and $\mathbf{M}_\theta = M_\theta \boldsymbol{\mu}$ as a system of active forces as well as the reaction forces $\mathbf{N} = N\mathbf{k}$, $\mathbf{R}_\lambda = R_\lambda \boldsymbol{\lambda}$, and $\mathbf{R}_\mu = R_\mu \boldsymbol{\mu}$ applied to the disk from the plane. Here, $\mathbf{g} = -g\mathbf{k}$, g is the gravity acceleration, $\mathbf{N}$ is the normal reaction force, and $\mathbf{R}_\lambda$ and $\mathbf{R}_\mu$ are components of the Coulomb dry-friction force. By the torques $\mathbf{M}_\phi$, $\mathbf{M}_\psi$, and $\mathbf{M}_\theta$ the disk motion control is performed and these torques are often referred to in the literature as the directional torque, pedalling torque, and tilting (also called side inclination) torque, respectively. The position of the disk with respect to the inertial frame $Oxyz$ is determined by the four Lagrangean coordinates x_G, y_G, ϕ, and ψ.

The angular velocity of the disk can be expressed as:

$$\boldsymbol{\omega} = -\dot{\psi}\boldsymbol{\lambda} + \dot{\phi}\boldsymbol{\nu} = -\dot{\psi}\sin\phi\boldsymbol{i} + \dot{\psi}\cos\phi\boldsymbol{j} + \dot{\phi}\boldsymbol{k}, \tag{2.1}$$

where an overdot denotes the derivative with respect to time t. The condition of non-slipping of the disk is expressed as the following velocity constraint:

$$\mathbf{v}_C = 0, \tag{2.2}$$

where $\mathbf{v}_C$ is the velocity of the contact point C of the disk with the plane Oxy. Further, the velocity of the mass center G of the disk can be written out in the following two equivalent ways:

$$\mathbf{v}_G = \dot{x}_G\mathbf{i} + \dot{y}_G\mathbf{j} \tag{2.3}$$

and

$$\mathbf{v}_G = \mathbf{v}_C + \boldsymbol{\omega} \times \mathbf{r}_{C/G} = r\dot{\psi}\cos\phi\mathbf{i} + r\dot{\psi}\sin\phi\mathbf{j} \tag{2.4}$$

where $\mathbf{r}_{C/G} = r\mathbf{k}$ is the position vector of the point G relative to the point C. Equating the relations (2.3) and (2.4) yields the following nonholonomic constraints:

$$\dot{x}_G = V\cos\phi, \tag{2.5}$$

$$\dot{y}_G = V \sin\phi, \tag{2.6}$$

where V is a quasi-velocity [6] introduced as:

$$r\dot{\psi} = V. \tag{2.7}$$

The Newton-Euler equations [4, 6, 7, 23] of the disk read:

$$m\dot{\mathbf{v}}_G = \mathbf{N} + \mathbf{R}_\mu + \mathbf{R}_\lambda - mg\mathbf{k}, \tag{2.8}$$

$$\dot{\mathbf{L}}_G = -\mathbf{r}_{C/G} \times \mathbf{R}_\lambda - \mathbf{r}_{C/G} \times \mathbf{R}_\mu + \mathbf{M}_\phi + \mathbf{M}_\psi + \mathbf{M}_\theta, \tag{2.9}$$

where $\mathbf{L}_G$ is the angular momentum of the disk about the mass center G [6, 23] expressed in the moving frame $G\xi\eta\zeta$ as:

$$\mathbf{L}_G = -I_\xi\dot{\psi}\boldsymbol{\lambda} + I_\zeta\dot{\phi}\boldsymbol{\nu}, \tag{2.10}$$

where $I_\xi = (1/2)mr^2$ and $I_\zeta = (1/4)mr^2$ are the mass moments of inertia of the disk about the axes ξ and ζ, respectively. Since the velocity $\mathbf{v}_G$ can be expressed in the frame $G\xi\eta\zeta$ as:

$$\mathbf{v}_G = V\boldsymbol{\mu}, \tag{2.11}$$

then using the obvious relations $\dot{\boldsymbol{\lambda}} = \dot{\phi}\boldsymbol{\mu}$ and $\dot{\boldsymbol{\mu}} = -\dot{\phi}\boldsymbol{\lambda}$ yields:

$$\dot{\mathbf{v}}_G = -V\dot{\phi}\boldsymbol{\lambda} + \dot{V}\boldsymbol{\mu}, \tag{2.12}$$

$$\dot{\mathbf{L}}_G = -I_\xi\ddot{\psi}\boldsymbol{\lambda} - I_\xi\dot{\phi}\dot{\psi}\boldsymbol{\mu} + I_\zeta\ddot{\phi}\boldsymbol{\nu}. \tag{2.13}$$

Note that mass moments of inertia I_ξ and I_ζ represent constant scalar quantities. Finally, based on the expressions (2.7), (2.12), and (2.13), from Eqs. (2.8) and (2.9) it can be obtained the following differential equations of motion of the disk :

$$-mV\dot{\phi} = R_\lambda, \tag{2.14}$$

$$m\dot{V} = R_\mu, \tag{2.15}$$

$$0 = N - mg, \tag{2.16}$$

$$-I_\xi\frac{\dot{V}}{r} = R_\mu r - M_\psi, \tag{2.17}$$

$$-I_\xi\dot{\phi}\frac{V}{r} = M_\theta - R_\lambda r, \tag{2.18}$$

$$I_\zeta\ddot{\phi} = M_\phi. \tag{2.19}$$

Note that the differential equations (2.14)–(2.19) could have been also obtained by using various forms of differential equations for the non-holonomic systems (see for more details e.g., [24]). However, using general theorems of dynamics is more convenient in this case than using different methods and procedures of analytical mechanics with multipliers of constraints because, here, the Coulomb dry friction force is obtained directly, expressed via coordinates and their derivatives, which is necessary for setting up the Coulomb condition, in order that slip does not occur. In the procedures of analytical mechanics, after determination of the multipliers, it is also necessary to show their nature, and this can be done again only by comparison to the equations obtained by general theorems, as has been done in [24]. Solving Eqs. (2.14)–(2.19) for the control torques M_ψ, M_θ, and M_ϕ yields:

$$M_\psi = \tfrac{3}{2} mr\dot{V}, \tag{2.20}$$

$$M_\theta = -\tfrac{3}{2} mrV\dot{\phi}, \tag{2.21}$$

$$M_\phi = \tfrac{1}{4} mr^2\ddot{\phi}. \tag{2.22}$$

Finally, it should be pointed out that the condition of the realizability of the condition of roll without slip in presence of the Coulomb dry-friction forces requires the fulfillment of the following inequality:

$$R_\lambda^2 + R_\mu^2 \leqslant k_f^2 N^2 \tag{2.23}$$

where k_f is the coefficient of dry friction.

3. The brachistochronic rolling of the disk under the sufficiently large coefficient of dry friction k_f

Let us assume that the disk shown in Fig. 2 is rolling without slip and that the the coefficient of dry friction, k_f, during the motion of the disk has such values for which the condition (2.23) is satisfied. Since it is a well-known fact that the brachistochronic motion of mechanical systems is realized by control forces whose power is equal to zero, then the power of control torques $\mathbf{M}_\phi$, $\mathbf{M}_\psi$, and $\mathbf{M}_\theta$ must be equal to zero, that is:

$$P_w \equiv M_\phi\dot{\phi} + M_\psi\dot{\psi} = 0. \tag{3.1}$$

Note that motions of mechanical systems from one to another specified configuration for a minimum time, where the power of control forces does not equal zero (see e.g., [25, 26]) are referred to as the optimum time motions or minimum time motions. Also, more details about the choice of control forces for realization of the brachistochronic motion of mechanical systems can be found in [27]. Hence, during the brachistochronic motion of the disk, the principle of conservation of energy holds:

$$\tfrac{1}{2} m\big(\dot{x}_G^2 + \dot{y}_G^2\big) + \tfrac{1}{2} I_\xi\dot{\psi}^2 + \tfrac{1}{2} I_\zeta\dot{\phi}^2 = T_0 \tag{3.2}$$

where T_0 is the kinetic energy of the disk at the initial instant $t_0 = 0$. Introducing one more quasi-velocity in the following way:

$$\varOmega = \dot{\phi} \tag{3.3}$$

and using the relations (2.5), (2.6), (2.7), and (3.3), the relation (3.2) may be written in the following form:

$$V^2 + \frac{r^2\varOmega^2}{6} = c_1^2 \tag{3.4}$$

where $c_1^2 = 4T_0/(3m)$. Let us now introduce control variables in the following way:

$$u_1 = V, \quad u_2 = \Omega. \tag{3.5}$$

Using these control variables, the relations (2.5), (2.6), and (3.3) take the form of state equations of the problem considered as follows:

$$\dot{x}_G = u_1 \cos\phi, \tag{3.6}$$

$$\dot{y}_G = u_1 \sin\phi, \tag{3.7}$$

$$\dot{\phi} = u_2, \tag{3.8}$$

whereas the relation (3.2) becomes:

$$u_1^2 + \frac{r^2 u_2^2}{6} - c_1^2 = 0. \tag{3.9}$$

The brachistochrone problem of the disk, whose state equations are determined by Eqs. (3.6)–(3.8), consists in determining the controls u_1 and u_2 and the state variables x_G, y_G, and ϕ corresponding to them, so that the disk starting from the initial position in which one has:

$$t_0 = 0,\ x_G(t_0) = 0,\ y_G(t_0) = 0,\ \phi(t_0) = 0, \tag{3.10}$$

reaches the terminal position where:

$$t = t_f,\ x_G(t_f) = a,\ y_G(t_f) = a,\ \phi(t_f) = \frac{\pi}{2}, \tag{3.11}$$

for the minimum time t_f where a is a given constant. This can be expressed as the minimization of the objective function:

$$J = \int_0^{t_f} dt \to \min \tag{3.12}$$

subject to (3.6)–(3.9) where t_f is free. To solve the optimal control problem formulated by Pontryagin's maximum principle [28–32], the Hamiltonian is formed:

$$H = -1 + u_1(\lambda_x \cos\phi + \lambda_y \sin\phi) + \lambda_\phi u_2 + \mu\Big(u_1^2 + \frac{r^2 u_2^2}{6} - c_1^2\Big), \tag{3.13}$$

where λ_x, λ_y, and λ_ϕ are the costate variables and μ is the Lagrange multiplier. The corresponding costate equations read:

$$\dot{\lambda}_x = -\frac{\partial H}{\partial x} = 0 \ \Rightarrow\ \lambda_x = \text{const.}, \tag{3.14}$$

$$\dot{\lambda}_y = -\frac{\partial H}{\partial y} = 0 \ \Rightarrow\ \lambda_y = \text{const.}, \tag{3.15}$$

$$\dot{\lambda}_\phi = -\frac{\partial H}{\partial \phi} = u_1(\lambda_x \sin\phi - \lambda_y \cos\phi). \tag{3.16}$$

Further, in accordance with the theory of optimal control, the necessary conditions of optimality of the Hamiltonian H with respect to the controls u_1 and u_2 are:

$$\frac{\partial H}{\partial u_1} = 0 \ \Rightarrow\ \lambda_x \cos\phi + \lambda_y \sin\phi + 2\mu u_1 = 0, \tag{3.17}$$

$$\frac{\partial H}{\partial u_2} = 0 \ \Rightarrow\ \lambda_\phi + \frac{\mu r^2}{3} u_2 = 0. \tag{3.18}$$

Since the transversality condition associated with the time t_f is:

$$H(t_f) = 0 \tag{3.19}$$

and that the Hamiltonian H is not an explicit function of time t, then one has that:

$$H(t) \equiv 0, \quad \forall t \in [0, t_f], \tag{3.20}$$

which, based on Eqs. (3.17), (3.18), and (3.18), yields:

$$1 + 2\mu c_1^2 = 0. \tag{3.21}$$

Solving the equations system (3.17), 3.18, and (3.21) for u_1, u_2, and μ yields:

$$u_1 = c_1^2(\lambda_x \cos\phi + \lambda_y \sin\phi), \tag{3.22}$$

$$u_2 = \frac{6c_1^2\lambda_\phi}{r^2}, \tag{3.23}$$

$$\mu = -\frac{1}{2c_1^2}. \tag{3.24}$$

Finally, the brachistochrone problem posed, in accordance with the above relations, is reduced to solving a system of four first-order differential equations of the form:

$$\dot{x}_G = c_1^2(\lambda_x \cos\phi + \lambda_y \sin\phi)\cos\phi, \tag{3.25}$$

$$\dot{y}_G = c_1^2(\lambda_x \cos\phi + \lambda_y \sin\phi)\sin\phi, \tag{3.26}$$

$$\dot{\phi} = \Omega, \tag{3.27}$$

$$\dot{\Omega} = \frac{6c_1^4}{r^2}(\lambda_x \cos\phi + \lambda_y \sin\phi)(\lambda_x \sin\phi - \lambda_y \cos\phi), \tag{3.28}$$

Taking that $r = \sqrt{6}\,\mathrm{m}$, $c_1^2 = 1\,\mathrm{m^2/s^2}$, $g = 9.80665\,\mathrm{m/s^2}$, and $a = 1\,\mathrm{m}$, in solving the equations system (3.25)–(3.28) by the shooting method [33] one starts from the values $t_0 = 0$, $x_G(0) = 0$, $y_G(0) = 0$, $\phi(0) = 0$, $\Omega(0) = \sqrt{1-\lambda_x^2}$ (the case considered is $\dot{\phi}(0) > 0$), where shooting of the values $x_G(t_f) = 1\,\mathrm{m}$, $y_G(t_f) = 1\,\mathrm{m}$, and $\phi(t_f) = \pi/2$ is performed by choosing the values $t_f > 0$, λ_x, and λ_y. Note that for the initial and terminal instants of motion, from the relation (3.9) it follows that $|\lambda_x| \leqslant 1$ and $|\lambda_y| \leqslant 1$. In this manner, using the built-in functions *NDSolve* and *First* in the Mathematica program package [34], the following dependencies can be established in a numerical form: $x_G(t_f) - 1 \equiv h_x(t_f, \lambda_x, \lambda_y)$, $y_G(t_f) - 1 \equiv h_y(t_f, \lambda_x, \lambda_y)$, and $\phi(t_f) - \pi/2 \equiv h_\phi(t_f, \lambda_x, \lambda_y)$. Now, based on (3.11), the following system of nonlinear equations can be found:

$$h_x(t_f, \lambda_x, \lambda_y) = 0, \tag{3.29}$$

$$h_y(t_f, \lambda_x, \lambda_y) = 0, \tag{3.30}$$

$$h_\phi(t_f, \lambda_x, \lambda_y) = 0. \tag{3.31}$$

Solving the system of equations (3.29)–(3.31) by using the built-in Mathematica function *FindRoot* (see [34]) yields $t_f = 2.21171\,\mathrm{s}$ and $\lambda_x = \lambda_y = 0.543895\,\mathrm{s/m}$. Based on these data, the corresponding graphs are shown in Figs. 3, 4, 5, and 6.

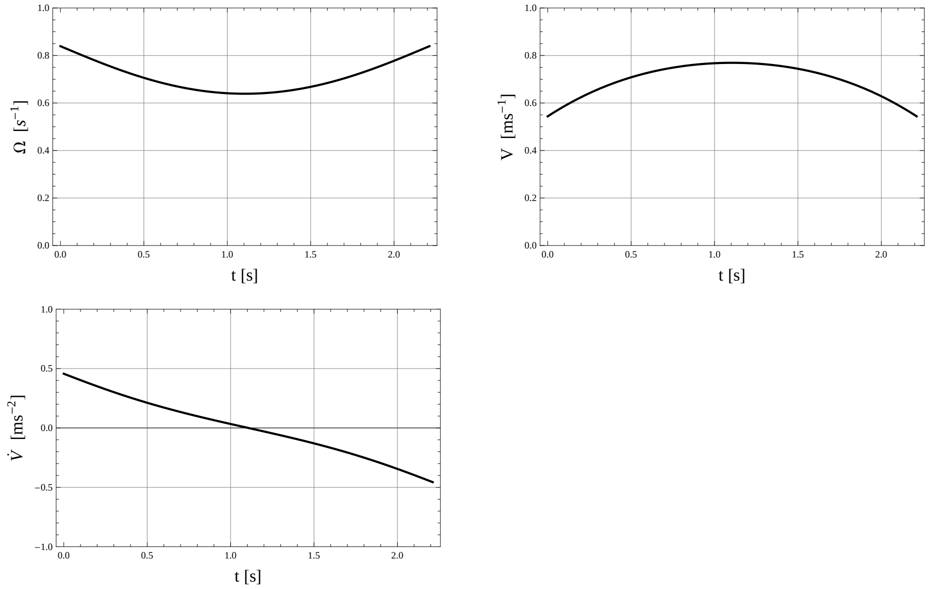

FIGURE 3. Graphs of the functions $\Omega(t)$, $V(t)$, and $\dot{V}(t)$ versus time.

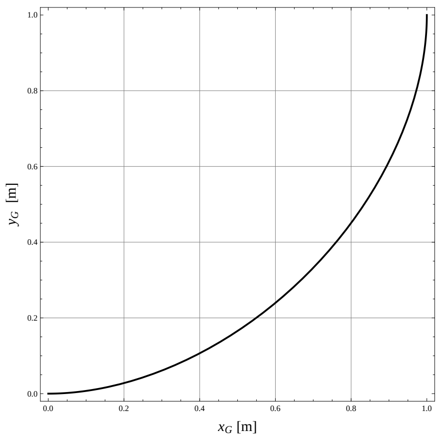

FIGURE 4. Trajectory of the mass center G of the disk (graph of the contact loci L.

Also, each of the dependencies (3.29)–(3.31) can be graphically represented in a t_f, λ_x, λ_y-space using the built-in Mathematica function *ContourPlot3D* (see [**34**]) as shown in Fig. 7. At the intersection of the surfaces there is the obtained solution of the system of nonlinear equations (3.29)–(3.31).

By observing Fig. 7 it can be concluded that the obtained solution represents the global minimum time for the brachistochronic motion of the disk. The problem

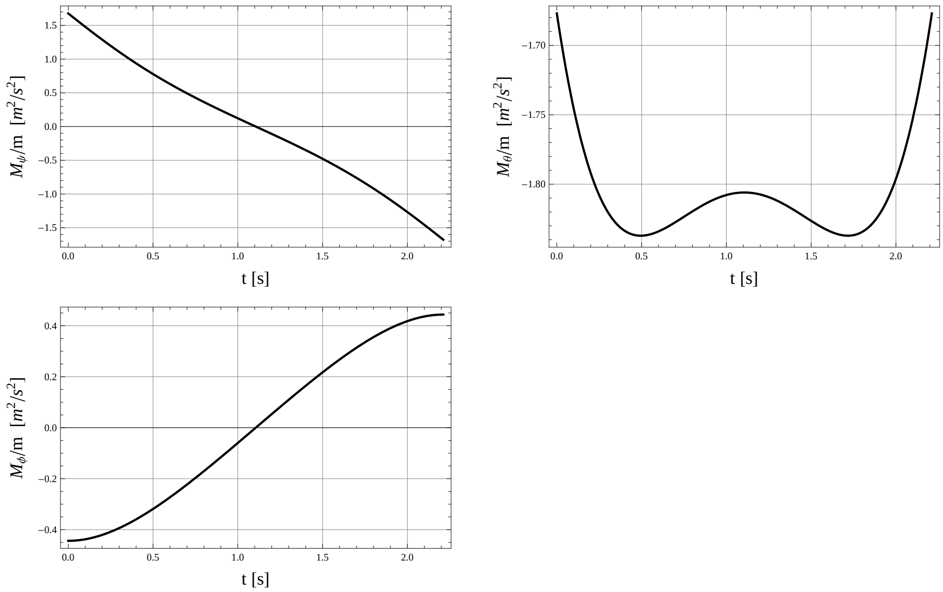

FIGURE 5. Magnitudes of the torques $\mathbf{M}_\psi$, $\mathbf{M}_\theta$, and $\mathbf{M}_\phi$ scaled with m versus time.

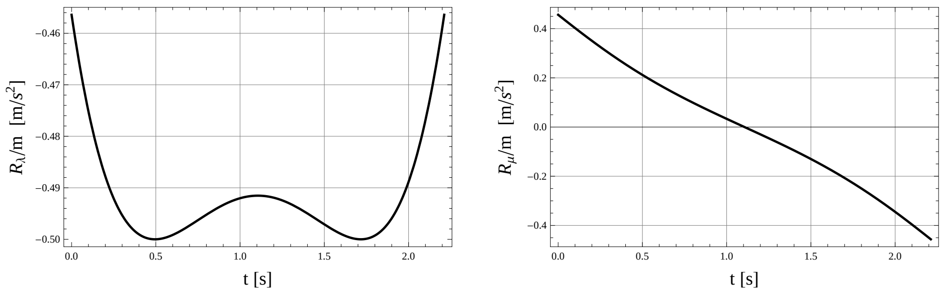

FIGURE 6. Magnitudes of the forces $\mathbf{R}_\lambda$ and $\mathbf{R}_\mu$ scaled with m versus time.

of determining the global minimum time of the brachistochronic motion of mechanical systems can be found in more detail in [35, 36]. Further, it is noticeable from Fig. 3 that $V > 0$ and $\Omega > 0$, which means that in the considered brachistochronic motion the angles ϕ and ψ represent monotonically increasing functions of the time t. Note that in this section it is assumed that during the brachistochronic motion of the disk the value of the coefficient k_f is such that the following inequality is fulfilled:

$$k_f \geqslant F(t) \equiv \sqrt{\frac{V^2\dot{\phi}^2 + \dot{V}^2}{g^2}} \equiv \frac{\sqrt{\Omega^2(\lambda_x^2 + \lambda_y^2)}}{g} \tag{3.32}$$

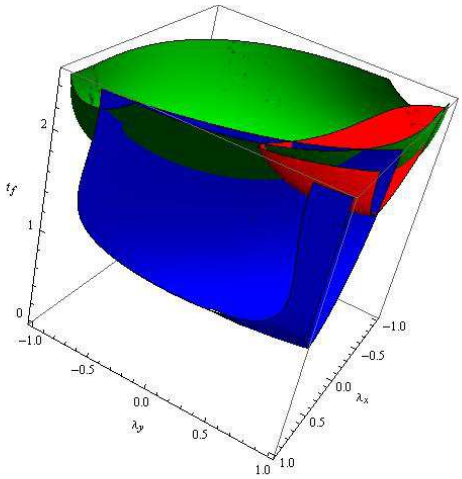

FIGURE 7. Crossing of surfaces $h_x(t_f, \lambda_x, \lambda_y) = 0$, $h_y(t_f, \lambda_x, \lambda_y) = 0$, and $h_\phi(t_f, \lambda_x, \lambda_y) = 0$.

which, by using the relations (3.3), (3.5), and (3.22), follows directly from the inequality (2.23). The graph of the function $F(t)$ during the time interval $[0, t_f]$ is shown in Fig. 8 where $F_{\max} = F(0) = F(t_f) = 0.065819$.

This graph is used to evaluate the coefficient k_f for which it is possible to realize previously determined brachistochronic motion of the disk by the Coulomb dry-friction forces. Thus, the qualitative analysis of Fig. 8 can distinguish the following three characteristic cases: for value $k_{f1} > F_{\max}$ the inequality (3.32) is satisfied over the entire interval $[0, t_f]$ (the case considered in this section); for value $F_{\min} < k_{f2} < F_{\max}$ the inequality (3.32) is disturbed on the initial and terminal sub-interval of the interval $[0, t_f]$; for value $k_{f3} < F_{\min}$ the inequality (3.32) is disturbed over the entire interval $[0, t_f]$. The section below will analyze the case when $k_f = k_{f2}$.

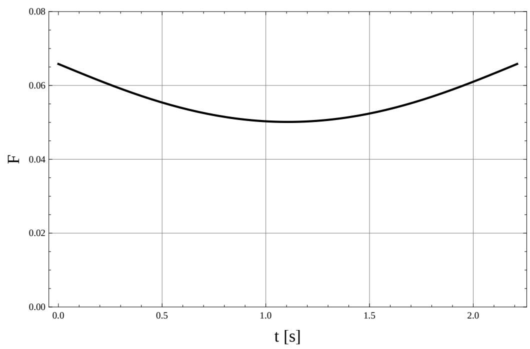

FIGURE 8. Graph of the function $F(t)$ versus time.

4. The brachistochronic rolling of the disk under the small coefficient of dry friction k_f

Now, consider the situation when $k_f = k_{f2}$ (see the discussion at the end of Section 3). Based on the qualitative analysis of Fig. 8, the brachistochronic motion of the disk will be determined for this case in such way as to take that control moments change, so that on the initial and terminal part of the interval of motion the relation (3.32) is satisfied as an equality, while in the middle part of the interval of motion this relation is satisfied as an inequality. In this sense, let us introduce the following two control variables u_1 and u_2 as follows:

$$\dot{\phi} = u_1, \quad \dot{V} = u_2. \tag{4.1}$$

In accordance with the introduced control variables, the following state equations will be considered:

$$\dot{x}_G = V\cos\phi, \tag{4.2}$$

$$\dot{y}_G = V\sin\phi, \tag{4.3}$$

$$\dot{\phi} = u_1, \tag{4.4}$$

$$\dot{V} = u_2. \tag{4.5}$$

During the brachistochronic motion of the disk the following constraints are imposed (see (2.14), (2.15), (2.23), and (3.2)):

$$f_1 \equiv u_2^2 + V^2u_1^2 - k_f^2g^2 \leqslant 0, \tag{4.6}$$

$$f_2 \equiv V^2 + \frac{r^2u_1^2}{6} - c_1^2 = 0. \tag{4.7}$$

Now, the Hamiltonian corresponding to the considered brachistochronic motion of the disk can be written as [30, 32]:

$$H = -1 + \lambda_x V\cos\phi + \lambda_y V\sin\phi + \lambda_\phi u_1 + \lambda_V u_2 + \mu_1 f_1 + \mu_2 f_2 \tag{4.8}$$

where λ_x, λ_y, λ_ϕ, and λ_V are the costate variables and μ_1 and μ_2 are the Lagrange multipliers. In addition, for the Lagrange multiplier μ_1 one has [30, 32]:

$$\mu_1 \begin{cases} > 0, & f_1 = 0, \\ = 0, & f_1 < 0. \end{cases} \tag{4.9}$$

Thus, the costate equations read:

$$\dot{\lambda}_x = -\frac{\partial H}{\partial x} = 0 \ \Rightarrow\ \lambda_x = \text{const.}, \tag{4.10}$$

$$\dot{\lambda}_y = -\frac{\partial H}{\partial y} = 0 \ \Rightarrow\ \lambda_y = \text{const.}, \tag{4.11}$$

$$\dot{\lambda}_\phi = -\frac{\partial H}{\partial \phi} = V(\lambda_x\sin\phi - \lambda_y\cos\phi), \tag{4.12}$$

$$\dot{\lambda}_V = -\frac{\partial H}{\partial V} = -\lambda_x\cos\phi - \lambda_y\sin\phi - 2\mu_1 V u_1^2 - 2\mu_2 V, \tag{4.13}$$

whereas the necessary conditions of optimality of the Hamiltonian H with respect to the controls u_1 and u_2 read:

$$\frac{\partial H}{\partial u_1} = 0 \;\Rightarrow\; \lambda_\phi + \frac{\mu_2 r^2 u_1}{3} + 2\mu_1 V^2 u_1 = 0, \tag{4.14}$$

$$\frac{\partial H}{\partial u_2} = 0 \;\Rightarrow\; \lambda_V + 2\mu_1 u_2 = 0, \tag{4.15}$$

where the corresponding transversality conditions are:

$$\lambda_V(0) = 0, \qquad \lambda_V(t_f) = 0, \tag{4.16}$$

$$H(t_f) = 0. \tag{4.17}$$

As in Section 3, the transversality condition (4.17) and the fact that the Hamiltonian H is not an explicit function of time t implicate the relation (3.20). Based on the previous considerations and the qualitative analysis of the graph of function $F(t)$ shown in Fig. 8, the structure of the extremal trajectory defined in a parametric form as $x_G(t)$, $y_G(t)$, $\phi(t)$, $\psi(t)$ is:

$$\text{extremal trajectory} \begin{cases} \text{subarc } 1[0, t_1] & f_1 = 0, f_2 = 0, \\ \text{subarc } 2[t_1, t_2] & f_1 < 0, f_2 = 0, \\ \text{subarc } 3[t_2, t_f] & f_1 = 0, f_2 = 0, \end{cases} \tag{4.18}$$

where the instants t_1 and t_2 are the switching points of the extremal trajectory structure (4.18). In the intervals $[0, t_1]$ and $[t_2, t_f]$ from Eqs. (4.6) and (4.7) it follows that:

$$u_1 = \frac{\sqrt{6(c_1^2 - V^2)}}{r}, \tag{4.19}$$

$$u_2 = \pm\frac{\sqrt{k_f^2 g^2 r^2 - 6V^2(c_1^2 - V^2)}}{r}, \tag{4.20}$$

where in the interval $[0, t_1]$ the "+" sign should be taken in front of the square root in the expression (4.20) and the "−" sign in the interval $[t_2, t_f]$ (see Fig. 3). According to this, solving Eqs. (4.14) and (4.15) for μ_1 and μ_2 yields:

$$\mu_1 = \frac{-\lambda_V r}{\pm 2\sqrt{k_f^2 g^2 r^2 - 6V^2(c_1^2 - V^2)}}, \tag{4.21}$$

$$\mu_2 = -\frac{3\lambda_\phi}{r\sqrt{6(c_1^2 - V^2)}} + \frac{3\lambda_V V^2}{\pm r\sqrt{k_f^2 g^2 r^2 - 6V^2(c_1^2 - V^2)}}. \tag{4.22}$$

On the other hand, in the interval $[t_1, t_2]$ one has $\mu_1 = 0$ and, hence, from Eqs. (4.13), (4.14), and (4.15) it follows that:

$$\lambda_V(t) \equiv 0 \;\Rightarrow\; \dot{\lambda}_V(t) \equiv 0, \tag{4.23}$$

$$\lambda_\phi = -\frac{\mu_2 r^2 u_1}{3}, \tag{4.24}$$

$$2\mu_2 V = -(\lambda_x \cos\phi + \lambda_y \sin\phi). \tag{4.25}$$

Taking into account (4.8) and (4.18) and introducing the relations (4.23)–(4.25) into (3.20) yields:

$$\mu_2 = -\frac{1}{2c_1^2}. \tag{4.26}$$

Now, incorporating (4.26) into (4.24) and (4.25) gives:

$$V = c_1^2(\lambda_x \cos\phi + \lambda_y \sin\phi), \tag{4.27}$$

$$\lambda_\phi = \frac{\sqrt{6(c_1^2 - V^2)}}{c_1^2 r}, \tag{4.28}$$

where the expression (4.19) is used. Further, taking into account Eqs. (4.4) and (4.5) and taking time derivative of the expression (4.27) yields the expression for the control variable u_2 as:

$$u_2 = c_1^2\frac{\sqrt{6(c_1^2 - V^2)}}{r}(-\lambda_x \sin\phi + \lambda_y \cos\phi). \tag{4.29}$$

Finally, puting the expressions (4.19) and (4.27) into Eqs. (4.2)–(4.4) gives:

$$\dot{x}_G = c_1^2(\lambda_x \cos\phi + \lambda_y \sin\phi)\cos\phi, \tag{4.30}$$

$$\dot{y}_G = c_1^2(\lambda_x \cos\phi + \lambda_y \sin\phi)\sin\phi, \tag{4.31}$$

$$\dot{\phi} = \frac{\sqrt{6c_1^2[1 - c_1^2(\lambda_x \cos\phi + \lambda_y \sin\phi)^2]}}{r}. \tag{4.32}$$

Based on above considerations, the numerical procedure for determining the switching instants t_1 and t_2 as well as the time t_f of the brachistochronic motion of the disk consists of the following steps:

- In the interval $[0, t_1]$, by using the built-in Mathematica functions *NDSolve* and *First* with the initial conditions $x_G(0) = 0$, $y_G(0) = 0$, $\phi(0) = 0$, and $V(0) = V_0$, Cauchy's problem of the system of differential equations (4.2)—(4.5) is solved where Eqs. (4.19) and (4.20) are taken into account. Based on the expression (4.27), the following functional dependence in a numerical form, $V(t_1) - c_1^2(\lambda_x \cos\phi(t_1) + \lambda_y \sin\phi(t_1)) \equiv \Phi_1(V_0, t_1, \lambda_x, \lambda_y)$, is established.
- In the same interval, the backward integration of the differential equations (4.2)–(4.5) and (4.12)–(4.13) is performed, where $x_G(t_1)$, $y_G(t_1)$, $\phi(t_1)$, and $V(t_1)$ obtained in the first step are taken for the initial values as well as $\lambda_V(t_1) = 0$ and $\lambda_\phi(t_1) = \sqrt{6(c_1^2 - V^2(t_1))}/(c_1^2 r)$ (see Eqs. (4.23) and (4.28)). Thus, based on the transversality condition (4.16), the functional dependence in a numerical form, $\lambda_V(0) \equiv \Phi_2(V_0, t_1, \lambda_x, \lambda_y)$, is established.
- The integration of the differential equations (4.30)–(4.32) in the interval $[t_1, t_2]$, where the values $x_G(t_1)$, $y_G(t_1)$, and $\phi(t_1)$ obtained in the first step are taken for the initial values, is performed.
- The integration of the differential equations (4.2)–(4.5) and (4.12)–4.13 in the interval $[t_2, t_f]$, where the values $x_G(t_2)$, $y_G(t_2)$, and $\phi(t_2)$ obtained in the third step are taken for the initial values as well as $\lambda_V(t_2) = 0$ and $\lambda_\phi(t_2) = \sqrt{6(c_1^2 - V^2(t_2))}/(c_1^2 r)$ (see Eqs. (4.23) and (4.24)). Thus,

using the conditions (3.11) and the transversality condition (4.16) yields the following four functional dependencies in a numerical form: $x_G(t_f) - a \equiv \Phi_3(V_0, t_1, t_2, t_f, \lambda_x, \lambda_y)$, $y_G(t_f) - a \equiv \Phi_4(V_0, t_1, t_2, t_f, \lambda_x, \lambda_y)$, $\phi(t_f) - \pi/2 \equiv \Phi_5(V_0, t_1, t_2, t_f, \lambda_x, \lambda_y)$, and $\lambda_V(t_f) \equiv \Phi_6(V_0, t_1, t_2, t_f, \lambda_x, \lambda_y)$.

- The final step is solving the following system of nonlinear equations

$$\Phi_1(V_0, t_1, \lambda_x, \lambda_y) = 0, \tag{4.33}$$

$$\Phi_2(V_0, t_1, \lambda_x, \lambda_y) = 0, \tag{4.34}$$

$$\Phi_3(V_0, t_1, t_2, t_f, \lambda_x, \lambda_y) = 0, \tag{4.35}$$

$$\Phi_4(V_0, t_1, t_2, t_f, \lambda_x, \lambda_y) = 0, \tag{4.36}$$

$$\Phi_5(V_0, t_1, t_2, t_f, \lambda_x, \lambda_y) = 0, \tag{4.37}$$

$$\Phi_6(V_0, t_1, t_2, t_f, \lambda_x, \lambda_y) = 0 \tag{4.38}$$

for unknowns V_0, t_1, t_2, t_f, λ_x, and λ_y.

Thus, choosing $r = \sqrt{6}\,\mathrm{m}$, $c_1^2 = 1\,\mathrm{m}^2/\mathrm{s}^2$, $g = 9.80665\,\mathrm{m/s}^2$, $a = 1\,\mathrm{m}$, and $k_f = 0.0525$ and solving the system of equations (4.33)–(4.38) by using the built-in Mathematica function *FindRoot* (see [34]) yields $V_0 = 0.626499\,\mathrm{m/s}$, $t_1 = 1.08556\,\mathrm{s}$, $t_2 = 1.12776\,\mathrm{s}$, $t_f = 2.21333\,\mathrm{s}$, and $\lambda_x = \lambda_y = 0.546801\ \mathrm{s/m}$. The corresponding graphs are shown in Figs. 9, 10, and 11.

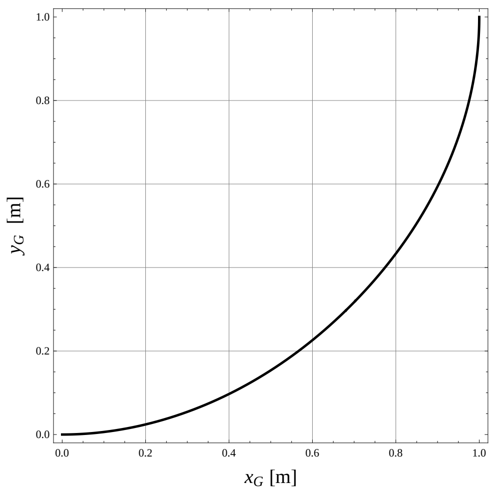

FIGURE 9. Trajectory of the mass center G of the disk for $k_f = k_{f2}$.

5. Conclusions

The analysis of the available literature leads to the conclusion that this paper presents new results related to the brachistochronic motion of the thin disk on a horizontal plane. It has been shown that the brachistochronic motion of the disk obtained in Section 3 cannot be realized for arbitrary values of the coefficient of

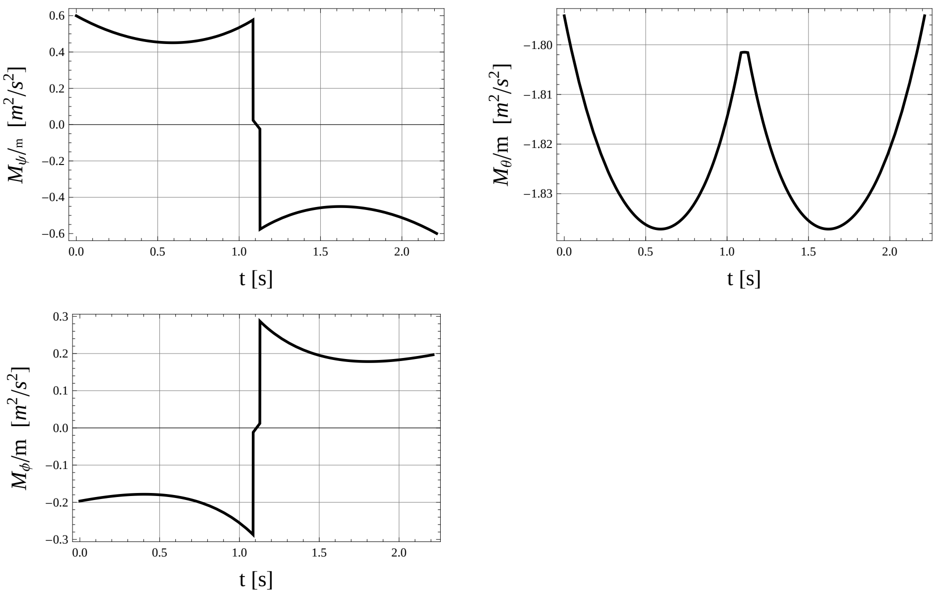

FIGURE 10. Magnitudes of the torques $\mathbf{M}_\psi$, $\mathbf{M}_\theta$, and $\mathbf{M}_\phi$ for $k_f = k_{f2}$ scaled with m versus time.

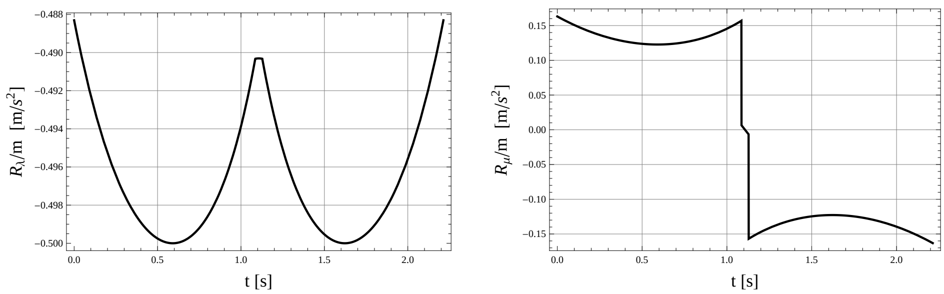

FIGURE 11. Magnitudes of the forces $\mathbf{R}_\lambda$ and $\mathbf{R}_\mu$ for $k_f = k_{f2}$ scaled with m versus time.

dry friction k_f. A specific range of values of the coefficient k_f requires the maintenance of the Coulomb friction force magnitude on a boundary value $k_f mg$ in the initial and terminal phase of the brachistochronic motion, using the corresponding laws of change in control torques M_ψ, M_θ, and M_ϕ. The approach proposed makes it possible to apply in analyzing the motion for some other combinations of boundary conditions (for example, $x_G(t_f) \neq y_G(t_f)$ and $\phi(t_f) \neq \pi/2$). Further considerations of the brachistochronic motion of the thin disk can be directed to the brachistochrone problem of the disk on an inclined plane surface as well as on curved surfaces.

Acknowledgements. The first author wishes to express his gratitude to the late Professors Josif Vuković and Vukman Čović for their useful suggestions and original ideas on the problem of the brachistochronic motion of nonholonomic mechanical systems with restrictions imposed by Coulomb's laws of friction.

References

1. E. T. Whittaker, *A Treatise on the Analytical Dynamics of Particles and Rigid Bodies*, Dover, New York, 1944.
2. L. A. Pars, *A Treatise on the Analytical Dynamics*, John Wiley & Sons, New York, 1968.
3. Ju. I. Neimark, N. A. Fufaev, *Dynamics of Nonholonomic Systems*, Am. Math. Soc., Providence, Rhode Island, 1972.
4. D.T. Greenwood, *Principles of Dynamics*, Prentice-Hall, Englewood Cliffs, New Jersey, 1988.
5. R. Cusman, J. Hermans, D. Kemppanien, *The Rolling Disc*, Prog. Nonlinear Differ. Equ. Appl. **19**, Birkhauser, 21–60, 1996.
6. H. Baruh, *Analytical Dynamics*, McGraw-Hill, Singapore, 1999.
7. H. Josephs, R. L. Huston, *Dynamics of Mechanical Systems*, CRC Press, Boca Ration, 2002.
8. A. M. Bloch, *Nonholonomic Mechanics and Control*, Springer-Verlag, New York, 2015.
9. Y. Yavin, C. Frangos, *Open loop strategies for the control of a disk rolling on a horizontal plane*, Comput. Methods Appl. Mech. Eng. **127** (1995), 227–240.
10. G. W. Ehlers, Y. Yavin, C. Frangos, *On the motion of a disc rolling on a horizontal plane: Path controllability and fedback control*, Comput. Methods Appl. Mech. Eng. **137** (1996), 345–356.
11. O. M. O'Reilly, *The dynamics of rolling disks and sliding disks*, Nonlinear Dyn. **10** (1996), 287–305.
12. Y. Yavin, *Inclination control of the motion of a rolling disk by using a rotor*, Comput. Methods Appl. Mech. Eng. **146**(3–4) (1997), 253–263.
13. Y. Yavin, *Stabilization and control of the motion of a rolling disk*, Math. Comput. Modelling **29** (1999), 45–54.
14. P. C. Paris, Li Zhang, *A disk rolling on a horizontal surface without slip*, Math. Comput. Modelling **36** (2002), 855–860.
15. L. Cui, J. S. Dai, *From sliding-rolling loci to instantaneous kinematics: An adjoint approach*, Mech. Mach. Theory **85** (2015), 161–171.
16. Y. Yavin, *Modelling of the motion of a disk rolling on a smooth rigid surface*, Appl. Math. Lett. **15** (2002), 815–818.
17. L. D. Akulenko, *An analog of the classical brachistochrone for a disk*, Dokl. Phys. **53** (2008), 156–159.
18. L. D. Akulenko, *Controlled rolling of a disc along a plane curve*, PMM, J. Appl. Math. Mech. **72** (2008), 660-668.
19. L. D. Akulenko, *The brachistochrone problem for a disc*, PMM, J. Appl. Math. Mech. **73** (2009), 371–378.
20. V. P. Legeza, *Brachistochrone for a rolling cylinder*, Mechanics of Solids **45** (2010), 27–33.
21. V. P. Legeza, *Conditions for pure rolling of a heavy cylinder along a brachistochrone*, Int. Appl. Mech. **46** (2010), 730–735.
22. A. Bakša, *Brachystochronous movement on a manifold*, Theor. Appl. Mech. **24** (1998), 1–11.
23. A. Bakša, *Rational Mechanics*, Lectures held at University of Belgrade Faculty of Mathematics in 1999/2000, Belgrade, 2000.
24. Sh. Kh. Soltakhanov, M. P. Yushkov, S. A. Zegzhda, *Mechanics of Non-holonomic Systems: A New Class of Control Systems*, Springer-Verlag, Berlin Heidelberg, 2009.
25. R. S. Chowdhry, E. M. Cliff, *Optimal rigid body motions, Part 2: Minimum time solutions*, The Journal of Optimization Theory and Applications **70**(2) (1991), 255–276.
26. H. Shen, P. Tsiotras, *Time-optimal control of axi-symmetric rigid spacecraft using two controls*, J. Guid. Control Dyn. **22** (1999), 682–694.

27. V. Čović, M. Vesković, *Brachistochronic motion of a multibody system with Coulomb friction*, Eur. J. Mech., A, Solids **28**(4) (2009), 882–890.
28. L. S. Pontryagin, V. G. Boltyansky, R. V. Gamkrelidze, E. F. Mishchenko, *The Mathematical Theory of Optimal Processes*, Interscience Publishers, John Wiley and Sons, New York, 1962.
29. A. D. Ioffe, V. M. Tihomirov, *Theory of Extremal Problems*, Nauka, Moscow, 1974. (in Russian)
30. A. E. Bryson, Y. C. Ho, *Applied Optimal Control*, Hemisphere Publishing Corporation, New York, 1975.
31. V. M. Alekseev, V. M. Tihomirov, S. V. Fomin, *Optimal Control*, Nauka, Moscow, 1979. (in Russian)
32. D. G. Hull, *Optimal Control Theory for Applications*, Springer-Verlag, New York, 2003.
33. J. Stoer, J. Bulirsch, *Introduction to Numerical Analysis*, Springer, Berlin, 1993.
34. H. Ruskeepaa, *Mathematica Navigator: Mathematics, Statistics, and Graphics*, Academic Press, Burlington, 2009.
35. R. Radulović, A. Obradović, S. Šalinić, *Contribution to the determination of the global minimum time for the brachistochronic motion of a holonomic mechanical system*, Meccanica **52** (2017), 795–805.
36. R. Radulović, S. Šalinić, A. Obradović, S. Rusov, *A new approach for the determination of the global minimum time for the Chaplygin sleigh brachistochrone problem*, Math. Mech. Solids **22** (2017), 1462–1482.

БРАХИСТОХРОНО КРЕТАЊЕ ВЕРТИКАЛНОГ ДИСКА КОЈИ СЕ КОТРЉА БЕЗ КЛИЗАЊА ПО ХОРИЗОНТАЛНОЈ РАВНИ

Резиме. У раду се разматра брахистохроно кретање вертикалног танког хомогеног диска који се котрља без клизања по хоризонталној равни. Брахистохрони проблем је формулисан и решен у оквиру теорије оптималног управљања. Брахистохроним кретањем диска управља се са три спрега сила. За тако одређено брахистохроно кретање диска анализирана је могућност његове реализације у присуству Кулонове силе сувог трења. Такође, анализиран је утицај вредности коефицијента сувог трења на структуру екстремалне трајекторије. Дата су два илустративна нумеричка примера.

Department of Mechanics
Faculty of Mechanical Engineering
University of Belgrade
Belgrade
Serbia
aobradovic@mas.bg.ac.rs

(Received 02.10.2017.)
(Revised 24.11.2017.)
(Available online 30.11.2017.)

Department of Applied Mechanics, Mathematics and Physics
Faculty of Mechanical and Civil Engineering in Kraljevo
University of Kragujevac
Kraljevo
Serbia
salinic.slavisa@gmail.com

Department of Mechanics
Faculty of Mechanical Engineering
University of Belgrade
Belgrade
Serbia
rradulovic@mas.bg.ac.rs